THE ASTROPHYSICAL JOURNAL, IN PRESS
Preprint typeset using LaTeX style emulateapj v. 02/07/07

VLBA MEASUREMENT OF THE TRANSVERSE VELOCITY OF THE MAGNETAR XTE J1810–197

D. J. HELFAND,[1] S. CHATTERJEE,[2] W. F. BRISKEN,[3] F. CAMILO,[1] J. REYNOLDS,[4] M. H. VAN KERKWIJK,[5] J. P. HALPERN,[1] AND S. M. RANSOM[6]

Received 2007 January 23; accepted 2007 March 12

ABSTRACT

We have obtained observations of the magnetar XTE J1810–197 with the Very Long Baseline Array at two epochs separated by 106 days, at wavelengths of 6 cm and 3.6 cm. Comparison of the positions yields a proper motion value of 13.5 ± 1.0 mas yr^{-1} at an equatorial position angle of $209.^\circ4 \pm 2.^\circ4$ (east of north). This value is consistent with a lower-significance proper motion value derived from infrared observations of the source over the past three years, also reported here. Given its distance of 3.5 ± 0.5 kpc, the implied transverse velocity corrected to the local standard of rest is 212 ± 35 km s^{-1} (1σ). The measured velocity is slightly below the average for normal young neutron stars, indicating that the mechanism(s) of magnetar birth need not lead to high neutron star velocities. We also use Australia Telescope Compact Array, Very Large Array, and these VLBA observations to set limits on any diffuse emission associated with the source on a variety of spatial scales, concluding that the radio emission from XTE J1810–197 is $> 96\%$ pulsed.

Subject headings: stars: individual (XTE J1810–197) — stars: neutron — X-rays: stars — pulsars: general

1. INTRODUCTION

Neutron stars manifest the most extreme values of many stellar parameters including radius, density, surface temperature, rotation rate, magnetic field strength, and velocity. The relationships among these parameters are thought to provide constraints on such fundamental issues as the equation of state for matter at supra-nuclear densities and the conditions at the center of core-collapse supernovae. The connection between the final two properties, the inferred surface magnetic dipole field strength and the neutron star space velocity, has been debated for more than thirty years. Helfand & Tademaru (1977) first suggested a bimodal distribution of radio pulsar velocities and claimed a correlation between velocity and magnetic field strength. As the number of measured pulsar proper motions increased, data presented by Anderson & Lyne (1983) and Cordes (1986) debunked the bimodal distribution, but appeared to confirm the correlation between velocity and magnetic field strength, and Bailes (1989) explained it in the context of the formation of neutron stars in binary systems. As yet larger samples became available, the bimodality of the velocity distribution reappeared (cf. Narayan & Ostriker 1990; Lorimer et al. 1995; Cordes & Chernoff 1998; Brisken et al. 2003) — and once again disappeared (Hobbs et al. 2005; Faucher-Giguère & Kaspi 2006) — while the relationship between velocity and magnetic field strength was explained as an evolutionary difference in subpopulations rather than a physical connection between the origin of spin period, magnetic field strength, and velocity kick at birth (Cordes & Chernoff 1998).

Magnetars, first discussed by Duncan & Thompson (1992), were postulated to have the most extreme magnetic properties of all neutron stars with mean dipole field strengths ranging from $\sim 10^{14}$ to 10^{15} G, more than 100 times that of ordinary pulsars. Duncan and Thompson suggested that these high fields would form as a consequence of dynamo action in very rapidly rotating (spin period ~ 1 ms) proto-neutron stars. Magnetic braking in such stars would be extremely rapid, leading to the prediction of young, slowly rotating stars with very large magnetic dipole moments. The recognition of Anomalous X-ray Pulsars (AXPs) as a distinct class of neutron stars with periods of 5–12 s (Mereghetti & Stella 1995), and the confirmation of long rotation periods as a characteristic of Soft Gamma-ray Repeaters (SGRs; Kouveliotou 1999) led to a compelling argument, first suggested by Paczinski (1992), that these objects had very large magnetic fields, the decay of which powered their quiescent X-ray emission (Thompson & Duncan 1996).

Motivated by the large offset of the SGR 0526–66 from the center of its putative natal supernova remnant (SNR) N49 (Rothschild et al. 1994), as well as by the since discredited notion that normal gamma-ray bursts might originate in halo neutron stars, Duncan & Thompson (1992) suggested several mechanisms by which the high magnetic fields characteristic of magnetars would also lead to very high space velocities of $\sim 10^3$ km s^{-1}. These processes include asymmetric mass loss either at the time of collapse or in an anisotropic magnetized wind or jet, as well as anisotropic neutrino emission and/or the photon rocket effect. They noted that most of these mechanisms are ineffective for the normal pulsar population (although a few outliers of that population have velocities in excess of 10^3 km s^{-1}; Chatterjee et al. 2005). However, the recognition that AXPs and SGRs were both manifestations of magnetars, and that the former were, in several cases, centrally located in their natal SNRs, led Gaensler et al. (2001) to express skepticism regarding most proposed SGR/SNR associations and to conclude that magnetars as a class had velocities < 500 km s^{-1}.

Measurements of magnetar velocities thus provide an important clue regarding the AXP/SGR connection, as well as

[1] Columbia Astrophysics Laboratory, Columbia University, 550 West 120th Street, New York, NY 10027; djh@astro.columbia.edu, fernando@astro.columbia.edu, jules@astro.columbia.edu
[2] School of Physics A28, The University of Sydney, NSW 2006, Australia; S.Chatterjee@physics.usyd.edu.au
[3] National Radio Astronomy Observatory, PO Box 0, Socorro, NM 87801; wbrisken@aoc.nrao.edu
[4] Australia Telescope National Facility, CSIRO, Parkes Observatory, P.O. Box 276, Parkes, NSW 2870, Australia; John.Reynolds@atnf.csiro.au
[5] Department of Astronomy and Astrophysics, University of Toronto, 50 Saint George Street, Toronto, ON M5S 3H4, Canada; mhvk@astro.utoronto.ca
[6] National Radio Astronomy Observatory, 520 Edgemont Road, Charlottesville, VA 22903; sransom@nrao.edu

offering a diagnostic of the events accompanying the birth of magnetars including the generation of their extraordinary magnetic fields. Proper motion measurements are thus highly desirable. The high level of timing noise present in all magnetars with phase-connected timing solutions (see Woods & Thompson 2006, for a review, and Camilo et al. 2007a) renders a timing proper motion measurement impossible. To date, direct measurements have been prevented by the fact that the handful of known magnetars are distant, and are primarily detected at X-ray wavelengths where the angular resolution of the best telescope, *Chandra*, is $0\farcs5$; the few optical/infrared (IR) detections are very faint (e.g., Hulleman et al. 2000), making direct proper motion measurements difficult. Nonetheless, attempts are underway to measure proper motions in both of these wavelength regimes; in § 3 we describe such a measurement in IR for XTE J1810–197.

The transient AXP XTE J1810–197, with a rotation period of 5.54 s, was discovered following an increase in X-ray brightness by a factor of > 100 in early 2003 (Ibrahim et al. 2004), after which it began an exponential decay, heading to its pre-outburst level by 2007 (Gotthelf & Halpern 2007). It was then detected at IR wavelengths (Israel et al. 2004; Rea et al. 2004). Subsequently, Halpern et al. (2005) discovered that XTE J1810–197 was coincident with a radio source in the MAGPIS survey of the Galactic plane at 20 cm (Helfand et al. 2006). Followup observations with the Parkes telescope revealed XTE J1810–197 to be a bright radio pulsar with a number of unique properties (Camilo et al. 2006) including a flat spectrum, highly variable flux densities and pulse shapes at all frequencies from 0.3 GHz to 144 GHz and on all timescales from minutes to months, as well as having a very high degree of linear polarization ($> 95\%$; Camilo et al. 2007b).

The radio emission from XTE J1810–197 opens the possibility of using the Very Long Baseline Array (VLBA) to obtain the first magnetar proper motion. We report here our two-epoch measurement of the position of XTE J1810–197 which leads to the first measurement of a magnetar transverse velocity. In Section 2 we describe the VLBA observations, their reduction, and the proper motion determination. Section 3 describes a consistent IR proper motion measurement. Section 4 uses data from the Australia Telescope Compact Array (ATCA) and the Very Large Array (VLA), as well as the VLBA observations to set limits on any synchrotron nebula surrounding the magnetar. The final section summarizes the distance determinations for XTE J1810–197, derives the source velocity, and comments on the implications of the low value we find for the origin of magnetars.

2. VLBA OBSERVATIONS AND PROPER MOTION OF XTE J1810–197

We observed XTE J1810–197 with the NRAO VLBA on 2006 June 2 under an Exploratory Time request. While most radio pulsars are observed at 1.4 GHz, we took advantage of the extraordinarily flat spectrum of XTE J1810–197 ($S_\nu \propto \nu^{-\alpha}$, $\alpha \sim 0$; Camilo et al. 2006) to observe at 5 GHz and 8.4 GHz, where the VLBA offers both higher spatial resolution and better system temperatures; in addition, ionosphere-induced astrometric errors scale as ν^{-2}, and are thus greatly reduced at these higher frequencies, a benefit especially important for this low-declination source which must always be observed at low elevation angles. As is usual in astrometric projects where absolute positional information is required, the observations were phase-referenced by nodding back and forth between the target and a reference calibrator source, J1753–1843, which lies $\sim 4^\circ$ away. We used a cycle time of 90 s on the calibrator and 120 s on the target to ensure that visibility phase coherence was preserved. The bandwidth at both frequencies was 32 MHz for each of the L and R circular polarizations. The L and R correlation products were summed at imaging time to form total intensity. Linear polarization products (i.e., L $\times$ R) were not generated. A total of 58 minutes of on-source data was accumulated in each band using 2 s integration times.

While proper motion measurements benefit from long time baselines, the rapid decline in flux density observed for XTE J1810–197 (Camilo et al. 2007a) led us to acquire a second-epoch observation only 106 days later, on 2006 September 16, using identical observational parameters.

At both epochs and both frequencies, the VLBA correlator was gated using a pulse timing solution determined from observations at Nançay, Parkes, and the GBT (Camilo et al. 2007a) in order to boost the signal-to-noise ratio (S/N) for the magnetar. We employed a boxcar gate with a width of 4% of the pulse period, resulting in a S/N boost of $0.04^{-1/2} = 5$ (assuming all of the radio pulsed flux is captured in the gate window). Given the timing noise and pulse shape variability, especially at later epochs (Camilo et al. 2007a), the fraction of the pulsed emission actually captured in the gate is somewhat uncertain, although for the first epoch, the off-pulse image shows no sign of the source (see § 4.3).

The correlated data were reduced in AIPS using standard procedures. The visibility amplitudes were calibrated based on the measured system temperature at each antenna, and the target visibility phases, rates, and delays, as well as the bandpass responses, were calibrated using the observed visibility phases of the reference calibrator. We also included corrections for ionospheric propagation effects based on global models of the total electron content (TEC) in the Earth's ionosphere, which are derived every 2 hours from dual-frequency Global Positioning System measurements around the world[7]. Finally, the calibrated visibilities were transformed to create images, and astrometric positions were obtained at 5 GHz and 8.4 GHz by fitting Gaussians to the observed point source images. We detected XTE J1810–197 at both frequency bands and at both epochs; the first epoch detections were strong (S/N $\sim$ 75–150), while the second epoch detections had substantially lower S/N $\sim$ 6–7.

Along with the statistical uncertainty of these position measurements, two primary sources of systematic astrometric error remain in the calibrated data. First, the position of the reference calibrator J1753–1843 is known only to a precision of 4 mas (Petrov et al. 2006), which results not only in an absolute position offset (inconsequential for a proper motion measurement), but also increases slightly (~ 0.1 mas) the systematic errors in the data. Second, the southern declination of XTE J1810–197 implies a low elevation at all VLBA antennas, leading to increased atmospheric and ionospheric path lengths. Combined with the 4° separation between the calibrator and the target, this produces a substantial uncalibrated path differential, which is only partially corrected by the global TEC models. As illustrated in Chatterjee et al. (2004, Fig. 3), we expect the path differential to contribute systematic errors of ~ 1 mas to the astrometry at 5 GHz. Note that the angular separation between the target and calibrator is 4° in right ascension and 1° in declination, and the mismatch between positions derived at 5 GHz and 8.4 GHz is also substantially worse in right ascension, consistent with an ef-

[7] See ftp://cddis.gsfc.nasa.gov/gps/products/ionex .

TABLE 1
PARAMETERS FOR XTE J1810–197

Parameter	Value
Epoch	2006.42 (MJD 53888)
Right Ascension, α_0	$18^{\rm h}09^{\rm m}51\overset{\rm s}{.}08696$
Declination, δ_0	$-19^\circ 43' 51\overset{''}{.}9315$
μ_α (mas yr^{-1})	-6.60 ± 0.06
μ_δ (mas yr^{-1})	-11.72 ± 1.03
Proper motion, μ (mas yr^{-1})	13.5 ± 1.0
Equatorial p.a. (east of north)	$209\overset{\circ}{.}4 \pm 2\overset{\circ}{.}4$
Distance (kpc)	3.5 ± 0.5
$V_{\perp,{\rm LSR}}$[a] (km s^{-1})	212 ± 35
Galactic coordinates, l, b	$10\overset{\circ}{.}73, -0\overset{\circ}{.}16$

NOTE. — All astrometric parameters are in the J2000 equinox. Absolute positions are referenced to J1753–1843 (R.A. = $17^{\rm h}53^{\rm m}09\overset{\rm s}{.}088754$, Decl. = $-18^\circ 43' 38\overset{''}{.}52316$), which has a positional uncertainty of 4 mas. Our reported position for XTE J1810–197 is from the 8.4 GHz data at the first epoch, which has the lowest systematic errors, but the uncertainties encompass the position measured at 5 GHz as well (see § 2). Errors quoted are 1σ.

[a] This velocity in the plane of the sky has been corrected to the local standard of rest using the distance given, and values for the Galactic rotation velocity (assumed constant) and peculiar velocity of the Sun from Cox (2000).

fect similar to that observed by Chatterjee et al. (2004). Thus, even though the image S/N is highest for the first-epoch 5 GHz observations, the first-epoch 8.4 GHz data is less affected by residual ionospheric effects and leads to a better absolute position for XTE J1810–197, as listed in Table 1.

For a proper motion measurement, only the relative displacement (as shown in Fig. 1) is of importance, and so we fit independent proper motions to the positions in the two frequency bands. While this precludes a goodness of fit estimate, our measurements are dominated by systematic errors in any case. At 8.4 GHz, we measure a proper motion $\mu_\alpha = -6.54$ mas yr^{-1} and $\mu_\delta = -11.20$ mas yr^{-1}, while at 5 GHz, we measure $\mu_\alpha = -6.66$ mas yr^{-1} and $\mu_\delta = -13.78$ mas yr^{-1}. We combine these measurements as a weighted average, estimate our residual systematic errors from the scatter between the measurements, and add them in quadrature with the (smaller) statistical errors to derive our final uncertainties in the proper motion, as reported in Table 1.

3. MOTION OF THE INFRARED COUNTERPART

The IR source identified by Israel et al. (2004) on the basis of precise coincidence with the *Chandra* position and unusual colors is demonstrably the counterpart of XTE J1810–197 because of its variability (Rea et al. 2004). To the extent that we can measure it, the proper motion of the IR counterpart should therefore agree with the VLBA result. Here, we show that adaptive optics observations allow a proper motion to be measured, and that it is consistent. This method is therefore feasible for measuring or significantly constraining the proper motions of other magnetars, all of which are (thus far) radio quiet.

For this purpose, we used new and archival IR *K*-band observations. Specifically, we used a relatively wide-field image obtained with the near-IR imager NIRI on Gemini in 2003 September (2×2 arcmin^2), an image obtained with the adaptive optics system Altair on Gemini in 2006 September (22×22 arcsec^2), and two images obtained with the adaptive optics system NACO on the Very Large Telescope in 2004 March and September (27×27 arcsec^2). The reduction of these data followed basic steps, described in more detail in Camilo et al. (2007, in preparation).

We tied our observations to the International Celestial Reference System (ICRS) using 66 stars from the 2MASS catalog (Skrutskie et al. 2006) that had single, stellar counterparts on the NIRI image. Rejecting 8 outliers, the root-mean-square (rms) residuals per star were ~ 80 mas in each coordinate, consistent with the 2MASS measurement uncertainties. Using 37 fainter stars, we transferred this solution to the Altair image (with residuals per star of ~ 23 mas). Given the residuals in the two steps, our observations are tied to the 2MASS catalog to ~ 10 mas. We found that the counterpart was offset from the VLBA position derived in § 2 by $\Delta\alpha = -0\overset{''}{.}00$ and $\Delta\delta = -0\overset{''}{.}05$, which is well within the systematic uncertainty of $\lesssim 0\overset{''}{.}1$ with which the 2MASS catalog is tied to the ICRS (Skrutskie et al. 2006).

To determine proper motions, we measured centroids for 93 stars common to the three adaptive optics images. The proper motions thus measured depended in a systematic way on position, due to distortion. We corrected for differences in distortion in the different cameras by first obtaining quadratic, six-parameter fits for the proper motions of the stars as a function of offset in right ascension and declination relative to the position of XTE J1810–197. We then subtracted the fit corrections from the measured proper motions (this procedure ensures that the proper motion of XTE J1810–197 at this stage is relative to those of stars near it on the detectors). In order to place these proper motions on an absolute scale, we calculated the expected motions in this direction due to Galactic rotation and the peculiar motion of the Sun. We find that the former dominates for distances in excess of 1 kpc, and leads to proper motions in Galactic longitude ranging from -1 to -8 mas yr^{-1} between 1 kpc and 10 kpc, and declining thereafter. Roughly matching our observed relative proper motions to this (by applying a correction of -4 mas yr^{-1} in longitude and -0.5 mas yr^{-1} in latitude, and converting back to equatorial coordinates), we infer a proper motion for the counterpart of XTE J1810–197 of $\mu_\alpha = 1 \pm 4$ mas yr^{-1} and $\mu_\delta = -11 \pm 4$ mas yr^{-1} (see Fig. 2), where the quoted uncertainties are measurement errors and the systematic uncertainty is about 1 mas yr^{-1}. This is consistent at the 87% confidence level with the proper motion measured by VLBA (see Table 1).

4. LIMITS ON EXTENDED RADIO EMISSION

In the paper reporting the discovery of radio emission from XTE J1810–197, Halpern et al. (2005) argued, based on the source's non-detection in the Parkes multibeam pulsar survey (e.g., Manchester et al. 2001) and the tight limits on radio pulsations from other magnetars, that the radio source was likely arising as a result of diffuse synchrotron emission analogous to the wind nebulae seen around many young pulsars. While the detection of radio pulses at the X-ray rotation period demonstrated that we are presented with a new phenomenon, the presence of pulses does not rule out the existence of diffuse emission. We have thus explored this possibility using three separate instruments to probe for emission on linear scales from 5 AU to 0.5 pc.

4.1. *ATCA Observations*

XTE J1810–197 was observed with the ATCA in its 6D configuration simultaneously at 13 cm (2.368 GHz) and 20 cm (1.384 GHz) on 2006 June 8 under a Target of Opportunity request. At each frequency, for each of two orthogonal linear

polarizations, we sampled a bandwidth of 128 MHz split into 33 frequency channels. The array was used in a time-binning mode with visibilities recorded in 32 phase bins across the 5.54 s period. First, we observed the flux calibrator 1934–638. We then obtained data for approximately 7.5 hr, with scans of $\sim$20 min on the pulsar interspersed with $\sim$2 min scans on the phase calibrators 1730–130 and 1921–293.

The correlated data were analyzed using standard techniques with MIRIAD. In order to reduce the effects of confusion from the Galaxy, we discarded data at 20 cm with projected baselines $\leq$ 1170 m and data at 13 cm with projected baselines $\leq$ 150 m. The synthesized beam and rms at 20 cm were $19\farcs4 \times 4\farcs4$ and 0.19 mJy beam^{-1}, respectively. At 13 cm, the corresponding values were $15\farcs1 \times 3\farcs7$ and 0.17 mJy beam^{-1}. At each frequency, a map made from the four consecutive phase bins clearly containing the pulsar yielded a source consistent with the beam shape, with a pulse-averaged flux density of 8.5 mJy at both frequencies (hence implying a flat spectrum). Images constructed from the data in the remaining 28 phase bins show no source at the magnetar position. This implies a 2σ limit to any diffuse emission of $< 4\%$ of the measured average pulsed flux. Thus, on scales of approximately $5''$ to $30''$ ($\sim$0.1 to 0.5 pc), there is no evidence for any extended radio nebula surrounding XTE J1810–197. The 2σ limit on surface brightness implied by the 13 cm data is $\Sigma < 3.3 \times 10^{-21}$ W m^{-2} Hz^{-1} sr^{-1}.

4.2. *VLA Observations*

The fact that our first VLA followup observation at 3.6 cm showed that the source was 90% linearly polarized was an early indication that our initial hypothesis of an extended nebula was suspect. No gated VLA observations were made, and our best limit on diffuse emission associated with the source is from our 2006 April 3 observations at 3.6 cm first reported in Camilo et al. (2006); roughly 75 minutes of on-source data were recorded, yielding a map rms of 60 μJy beam^{-1}. The synthesized beam in the A-configuration for our *uv* coverage had a FWHM of $0\farcs34 \times 0\farcs17$. Fitting a two-dimensional Gaussian to the magnetar produced parameters wholly consistent with this beam shape. The source Gaussian plus a constant offset produced flux densities of 0.26, 0.16, and 0.10 mJy for nebula sizes of $1''$, $2''$, and $4''$, respectively. Thus, on scales of $1''$ to $5''$ (0.015 to 0.1 pc) excluding the pulsar location, any diffuse flux is $< 3\%$ of the pulsed value of 9.1 mJy on the date of the observation.

4.3. *VLBA Observations*

We can use the off-pulse data from the first-epoch VLBA observations to set a stringent limit on the unpulsed radio flux from XTE J1810–197 on smaller angular scales. The rms of the off-pulse 3.6 cm map at the magnetar location is 55 μJy beam^{-1} and the beam is 2.9 mas$\times$1.7 mas which corresponds to a linear size of about 4 AU. Since the on-pulse source flux density was 8.0 mJy on this day, this implies a 3σ limit of $< 2\%$ on any unpulsed emission associated with the neutron star itself; this is a conservative upper limit, as any miscentering of the pulse window as well as any emission far from the main pulse (as is seen on many occasions; Camilo et al. 2007a) will act to raise the rms in the off-pulse image. This result also rules out any diffuse emission on scales of 5 to 50 AU as bright as 0.05 to 5 mJy, although the latter is ruled out by the ATCA observations (§ 4.1) which fail to detect a point source in the off-pulse data an order of magnitude fainter.

Taken together, the three sets of observations both exclude significant off-pulse emission from the magnetar's magnetosphere and limit the fraction of flux in a diffuse surrounding nebula to $< 4\%$ of the pulsed flux on scales ranging from 5 AU to 0.5 pc. The faintest known pulsar wind nebulae (either isolated or inside a composite SNR) have $\Sigma \sim 3 \times 10^{-20}$ W m^{-2} Hz^{-1} sr^{-1} (see data in Green 2004). The limits reported here on scales of $\sim 5''$–$30''$ (§ 4.1) are a factor of 10 below this level and are therefore extremely constraining.

5. THE VELOCITY OF XTE J1810–197 AND IMPLICATIONS FOR MAGNETAR BIRTH

Prior to the discovery of radio emission from XTE J1810–197, magnetar distance estimates primarily were derived from X-ray absorption and the reddening along the line of sight (Durant & van Kerkwijk 2006), or from an associated SNR or star cluster. The radio detection adds two distance proxies that can be measured: a kinematical distance from HI absorption and the pulsar dispersion measure. Minter at al. (2007) provide a current review of all these determinations, concluding that the distance to XTE J1810–197 is 3.5 ± 0.5 kpc. We adopt this value in determining the transverse velocity of the magnetar.

Using the best value for the distance and the weighted average proper motion value (Table 1), the transverse velocity of the magnetar is 223 km s^{-1} uncorrected for differential Galactic rotation and solar motion. We have computed these corrections for a distance of 3.5 ± 0.5 kpc; the velocity with respect to the local standard of rest is $V_{\perp,\rm LSR} = 212 \pm 35$ km s^{-1} (1σ). In Galactic coordinates, the velocity vector has a position angle of $89\fdg5$ — i.e., its motion is directly along the Galactic plane.

This transverse velocity is comparable to the mean for the population of known normal radio pulsars (246 ± 22 km s^{-1}, according to Hobbs et al. 2005) and far below that of the fastest ordinary pulsars with direct proper motion and distance measurements ($V_\perp = 1100$ km s^{-1}; Chatterjee et al. 2005). For a random orientation of the three-dimensional velocity vector, it is likely that the space velocity is $\lesssim 400$ km s^{-1} (2σ). Despite all the striking characteristics of XTE J1810–197, its velocity is completely ordinary.

We can conclude from the foregoing that the generation of magnetar magnetic fields does not *require* that the forming neutron star acquire an extremely high velocity.

Given the large excursions observed in the period derivatives of magnetars, characteristic ages obtained from the spin parameters are unreliable. Nonetheless, given the association of some AXPs with SNRs, as well as the Galactic distribution of AXPs and SGRs, it is generally thought that these objects are young ($< 10^5$ yr). Given our well-constrained proper motion vector for XTE J1810–197, we can extrapolate back along its path for clues to its birth. There are no objects of interest within a cone representing 2×10^4 yr of motion (its characteristic age in 2007 February), but the location at $\approx 10^5$ yr (R.A. = $18^{\rm h}10^{\rm m}38^{\rm s}$, Decl. = $-19\fdg24'21''$) lies within the bounds of a very low surface brightness shell of radio emission (barely visible in the MAGPIS image[8]) approximately $15'$ in diameter (15 pc if at a distance of 3.5 kpc). The shell is not visible in either the MSX 20 μm image or the GLIMPSE 8 μm image, suggesting it is non-thermal. Since such shells cover a significant fraction of the Galactic plane near $b = 0^\circ$, this coincidence is at best weak evidence for an

[8] Available at http://third.ucllnl.org/cgi-bin/gpscutout .

association with the magnetar.

The peak flux density of XTE J1810–197 decreased by about an order of magnitude in late 2006 July and has shown no sign of recovery as of early 2007. Unless the radio brightness returns to its levels of early 2006, it will not be possible to measure a parallax. If the velocity of XTE J1810–197 is typical of the magnetar population, optical/IR and/or X-ray measurements to determine the proper motions of other magnetars will be challenging, but may still provide useful constraints.

The VLBA and VLA are telescopes operated by the National Radio Astronomy Observatory, a facility of the National Science Foundation operated under cooperative agreement by Associated Universities, Inc. The ATCA is part of the Australia Telescope, which is funded by the Commonwealth of Australia for operation as a National Facility managed by CSIRO. This research was supported in part by grants from the NSF to DJH (AST-05-07598) and FC (AST-05-07376); SC acknowledges support from the University of Sydney Postdoctoral Fellowship Program.

REFERENCES

Anderson, B., & Lyne, A. G. 1983, Nature, 303, 597
Bailes, M. 1989, ApJ, 342, 917
Brisken, W. F., Fruchter, A. S., Goss, W. M., Herrnstein, R. M., & Thorsett, S. E. 2003, AJ, 126, 3090
Camilo, F., Ransom, S. M., Halpern, J. P., Reynolds, J., Helfand, D. J., Zimmerman, N., & Sarkissian, J. 2006, Nature, 442, 892
Camilo, F., Cognard, I., Ransom, S. M., Halpern, J. P., Reynolds, J., Zimmerman, N., Gotthelf, E. V., Helfand, D. J., Demorest, P., Theureau, G., & Backer, D. C. 2007a, ApJ, submitted (astro-ph/0610685)
Camilo, F., Reynolds, J., Johnston, S., Halpern, J. P., Ransom, S. M., & van Straten, W. 2007b, ApJ, in press (astro-ph/0702616)
Chatterjee, S., Cordes, J. M., Vlemmings, W. H. T., Arzoumanian, Z., Goss, W. M., & Lazio, T. J. W. 2004, ApJ, 604, 339
Chatterjee, S., Vlemmings, W. H. T., Brisken, W. F., Lazio, T. J. W., Cordes, J. M., Goss, W. M., Thorsett, S. E., Fomalont, E. B., Lyne, A. G., & Kramer, M. 2005, ApJ, 630, L61
Cordes, J. M. 1986, ApJ, 311, 183
Cordes, J. M., & Chernoff, D. F. 1998, ApJ, 505, 315
Cox, A. N., ed. 2000, Allen's Astrophysical Quantities, 4th ed. (New York: AIP Press; Springer)
Duncan, R. C., & Thompson, C. 1992, ApJ, 392, L9
Durant, M., & van Kerkwijk, M. H. 2006, ApJ, 650, 1070
Faucher-Giguère, C.-A., & Kaspi, V. M. 2006, ApJ, 643, 332
Gaensler, B. M., Slane, P. O., Gotthelf, E. V., & Vasisht, G. 2001, ApJ, 559, 963
Gotthelf, E. V., & Halpern, J. P. 2007, in Isolated Neutron Stars: From the Interior to the Surface, ed. S. Zane, R. Turolla, & D. Page, in press (astro-ph/0608473)
Halpern, J. P., Gotthelf, E. V., Becker, R. H., Helfand, D. J., & White, R. L. 2005, ApJ, 632, L29
Helfand, D. J., & Tademaru, E. 1977, ApJ, 216, 842
Helfand, D. J., Becker, R. H., White, R. L., Fallon, A., & Tuttle, S. 2006, AJ, 131, 2525
Hulleman, F., van Kerkwijk, M. H., & Kulkarni, S. R. 2000, Nature, 408, 689
Hobbs, G., Lorimer, D. R., Lyne, A. G., & Kramer, M. 2005, MNRAS, 360, 974
Ibrahim, A. I., et al. 2004, ApJ, 609, L21
Israel, G. L., et al. 2004, ApJ, 603, L97
Kouveliotou, C. 1999, Proceedings of the National Academy of Science, 96, 5351
Lorimer, D. R., Lyne, A. G., & Anderson, B. 1995, MNRAS, 275, L16
Manchester, R. N., et al. 2001, MNRAS, 328, 17
Mereghetti, S., & Stella, L. 1995, ApJ, 442, L17
Minter, A. H., Camilo, F., Ransom, S. R., Zimmerman, N., Halpern, J. P., & Reynolds, J. 2007, ApJ, submitted
Narayan, R., & Ostriker, J. P. 1990, ApJ, 352, 222
Paczynski, B. 1992, Acta Astronomica, 42, 145
Petrov, L., Kovalev, Y. Y., Fomalont, E., & Gordon, D. 2006, AJ, 131, 1872
Rea, N., et al. 2004, A&A, 425, L5
Rothschild, R. E., Kulkarni, S. R., & Lingenfelter, R. E. 1994, Nature, 368, 432
Skrutskie, M. F., et al. 2006, AJ, 131, 1163
Thompson, C., & Duncan, R. C. 1996, ApJ, 473, 322
Woods, P. M., & Thompson, C. 2006, in Compact Stellar X-Ray Sources, ed. W. H. G. Lewin & M. van der Klis (Cambridge: Cambridge Univ. Press), 547

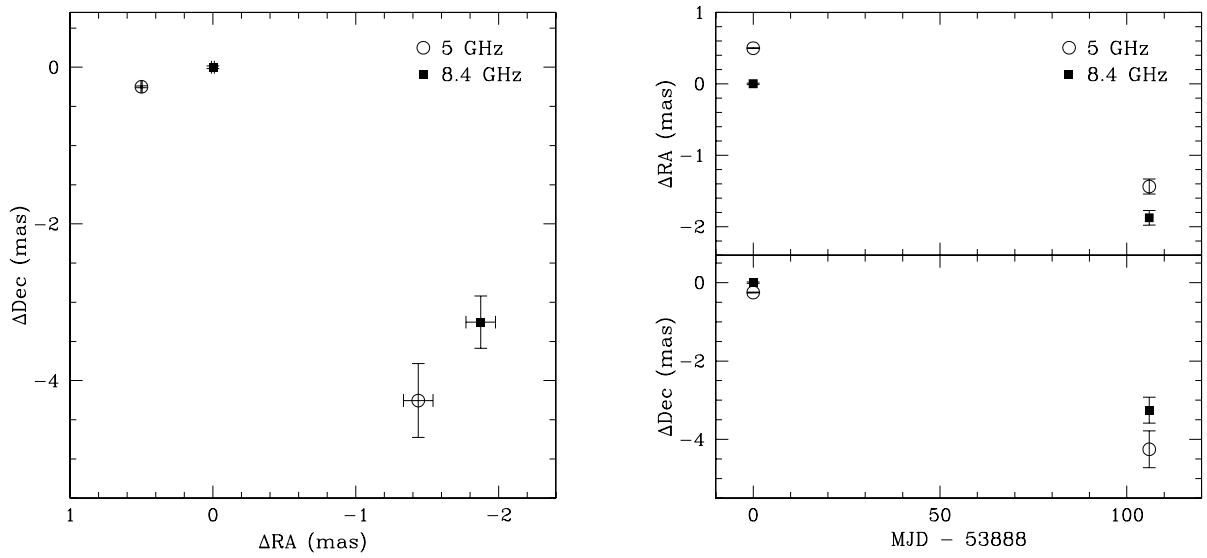

FIG. 1.— The proper motion of XTE J1810–197 using VLBA measurements. *Left*: Position offsets in right ascension and declination on MJD 53888 and MJD 53994, as measured with the VLBA at 5 GHz (*circles*) and 8.4 GHz (*solid squares*). Offsets are measured with respect to the 8.4 GHz position on MJD 53888, as listed in Table 1. *Right*: The same position offsets, shown as a function of time. The plotted error bars represent only the random position uncertainties, while the offset between the positions at different observing bands on the same day illustrates the residual systematic errors in the astrometry. The decrease in source flux density over time results in an increase in the random position error, and hence larger error bars, at the second epoch.

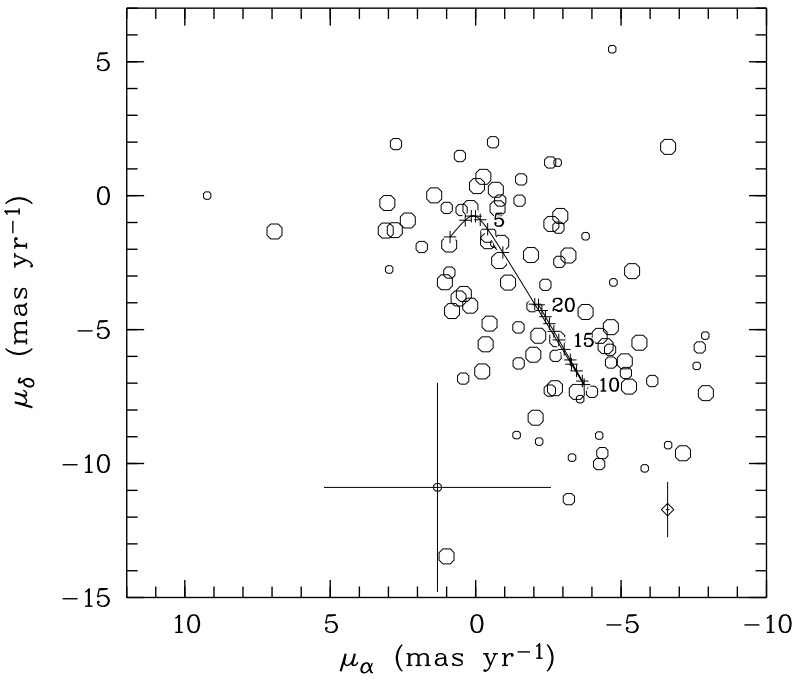

FIG. 2.— The proper motion of XTE J1810–197 (circle with error bars) derived from infrared observations relative to those for stars in the field (see § 3). The symbol sizes correspond to magnitude ranges, with, from large to small, $K < 20$, $20 < K < 21$, and $K > 21$, corresponding to proper-motion uncertainties of 0.7–1, 1–2, and 2.1–4 mas yr^{-1}, respectively. The proper motions were placed on an absolute scale by shifting them such that they matched the proper motions expected due to Galactic rotation (with an assumed constant velocity of 220 km s^{-1}) and solar peculiar velocity. These expectations are shown by the drawn curve for distances from 1 kpc to 20 kpc. The VLBA proper motion measurement (§ 2; Fig. 1) is shown by the diamond with error bars toward the bottom right of the plot.